Proceedings of the 21st ICSMGE, Vienna, Austria, 14 – 19 June 2026. Pistrol, Adam & Schweiger (eds.)
Published by: ÖGG, Austrian Society for Geomechanics, Salzburg, Austria, ISBN 978-3-9503898-4-5
https://doi.org/10.53243/ICSMGE2026-545

Image processing of desiccation crack patterns in a bentonite-sand mixture under wetting and drying cycles

Paniz Sourmanshahi, Pouya Alipanahi, **Hamed Sadeghi**, Farshad Yazdani
Department of Civil Engineering, Sharif University of Technology, Iran, hsadeghi@sharif.edu

ABSTRACT: Desiccation cracks in bentonite-sand mixtures pose significant challenges to engineered barriers such as landfill cover systems, high-level waste repositories, and cutoff walls. This study investigates the development and evolution of desiccation cracks under two wetting–drying (W–D) cycles. A 50:50 sand–bentonite mixture was compacted and exposed to two successive W–D cycles under the same conditions. High-resolution photographs of the soil surface during drying were taken and processed with an image-processing algorithm implemented in MATLAB. Total length, width distribution, and crack intensity factor (CIF) features were measured to monitor the temporal evolution of cracking. It is evident from the results that CIF rose from about 12% for the first cycle to more than 18% for the second cycle, which indicates the irreversibility and the cumulative nature of desiccation cracks. Even though the majority of crack growth occurred early in drying, subsequent cycles mainly contributed to the widening of the existing cracks rather than generating new ones. These findings revealed that desiccation cracking of the bentonite-sand barrier is cyclic-dependent and becomes more intense with W–D cycles. The image-based methodology proposed here presents an effective tool for crack severity determination relevant to long-term design and operation of geotechnical containment structures.

KEYWORDS: Bentonite-sand mixtures, Desiccation cracking, Wetting and drying cycles, Image processing, Crack intensity factor (CIF).

1 INTRODUCTION

Desiccation cracking is a widespread phenomenon in clay-rich soils and has been recognized as a critical issue in both geotechnical and environmental engineering (Tran et al., 2019). These cracks typically form due to moisture loss and shrinkage and significantly affect the hydro-mechanical behavior of soils (Namadi et al., 2020; Yazdani et al., 2024a; Julina and Thyagaraj, 2020). The emergence of crack networks facilitates preferential flow paths for water and solutes, increasing hydraulic conductivity and reducing the barrier function of soils (Gholami et al., 2025). When such cracking occurs in clay barriers used in waste containment systems, the protective function of these layers is compromised, increasing the likelihood of contaminant migration into the surrounding environment (Wan et al., 2018). In agricultural or natural settings, cracks cause rapid infiltration, leading to inefficient irrigation and deep soil erosion (Tang et al., 2012; Yazdani et al., 2024b). From a mechanical perspective, desiccation cracking results in strength loss, excessive deformation, and increased compressibility (Tang et al., 2018), contributing to slope failures and structural instability (Sadeghi et al., 2023). Preventing or reducing such cracking is therefore essential to maintain the long-term stability and performance of soil systems.

Bentonite-sand mixtures are widely recognized as engineered barrier materials in geoenvironmental applications due to their excellent sealing properties, cost-efficiency, and durability (Arabchobdar et al., 2024). These mixtures, consisting of granular sand and expansive bentonite clay, are commonly utilized in landfill liners, hydraulic buffers, and capping systems to limit fluid migration and protect surrounding environments (Ikeagwuani and Nwonu, 2019). The combination leverages bentonite's high swelling capacity, low hydraulic conductivity, and strong adsorption capabilities (Joshaghani and Ghasemi-Fare, 2021). The anisotropic permeability of bentonite-rich media must be carefully evaluated to ensure adequate performance in two-dimensional flow fields (Sadeghi et al., 2024). Bentonite-sand blends are particularly advantageous where high-quality natural clay is unavailable, allowing for the use of local sand materials. However, excessive bentonite content can lead to compaction difficulties due to coating effects on sand grains (Ruiz et al., 2012).

Understanding desiccation cracking mechanisms requires accurate characterization of the crack geometry and evolution over time. While traditional techniques such as manual measurement, transect-based intercept counting, and severity rating scales (Yu et al., 2021) provide basic insight, they often suffer from subjectivity, limited precision, and disturbance to the crack pattern. To overcome these limitations, digital image processing has become an increasingly reliable method for quantitatively analyzing surface crack networks in soils (Zhang et al., 2019).

Image analysis techniques allow for the accurate extraction of key geometrical parameters such as crack length, width, area, orientation, intensity (CIF), branching, and connectivity (Tang et al., 2008). Using software tools, two-dimensional images of cracked soil surfaces can be binarized and analyzed to compute crack metrics with high spatial resolution and repeatability. These metrics are essential for assessing hydraulic conductivity, pollutant transport, and structural integrity of soil liners and covers under wetting-drying (W-D) cycles. Moreover, image processing facilitates time-lapse analysis, which is critical for studying crack evolution as a dynamic and environmentally driven process (Sanchez et al., 2013; Cheng et al., 2020). Despite these advancements, current approaches predominantly investigate laboratory-generated crack patterns in uniform soils, a condition that may not adequately reflect field-scale heterogeneity or seasonal variations. Field investigations still face challenges related to complex geometries, surface disturbance, and variability in lighting or soil texture. Thus, refined and integrated approaches combining image-based methods with in situ environmental data, such as moisture content and temperature, are necessary to improve predictive models of cracking behavior (Yan et al., 2002).

A review of the existing literature reveals a lack of detailed investigation into crack characteristics, particularly crack length and width, under repeated W-D cycles. To address this gap, the present study aims to evaluate the effects of these cycles on the development of desiccation cracks. Experimental findings elucidate the progressive development of crack geometry, indicating that both crack length and width exhibit incremental growth with successive cycles. The use of image analysis proved to be an effective method for quantifying surface cracks. These findings offer valuable implications for geotechnical and environmental engineering applications, especially in the design and maintenance of landfill liners and

slopes, where crack formation can compromise structural integrity and long-term stability.

2 METHODS AND MATERIALS

2.1 *Soil properties*

In this study, a bentonite-sand mixture was prepared using two primary materials: commercially sourced bentonite and non-plastic sandy soil from Firuzkuh. To examine the effect of bentonite content, a soil mixture was formulated by blending bentonite with Firuzkuh sand at a target mass ratio of 50:50. This mixture was designated as B50, reflecting its bentonite mass fraction. The physical properties of the soil are summarized in Table 1. Figure 1 presents the grain-size distribution curve.

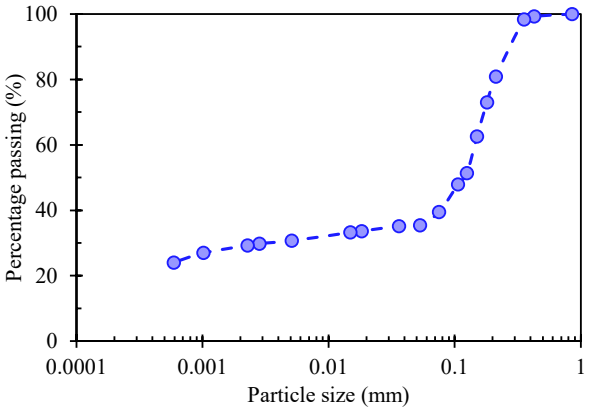

Figure 1. Grain-size distribution curves for the bentonite-sand mixture.

Table 1. Physical properties of the bentonite-sand mixture

Properties	Value
Specific gravity, G_s	2.59
Atterberg limits (%)	
Liquid limit, w_L	74.5
Plastic limit, w_P	23.5
Plastic Index, PI	51.0
Grain size distribution characteristics	
Mean grain size, D_{50} (mm)	0.120
Compaction characteristics	
Dry unit weight, $\gamma_{d\ max}$ (kN/m3)	14.86
Optimum water content, w_{opt} (%)	21.1

2.2 *Specimen preparation and test procedure*

Initially, cubic soil specimens with dimensions of 118 mm were compacted in eight successive layers. The relatively uniform distribution of void ratio along the sample height was guaranteed following the calculation based on the under-compaction method (Ladd, 1978; Sadeghi and Alipanahi, 2020). The samples were kept in a pond-like tank for a month to undergo a wetting cycle. The drying cycle was then continued until moisture equilibrium was reached. Following sample preparation, the specimens were subjected to repeated W-D cycles to simulate environmental conditions. Upon completion of each cycle, a photograph of the sample surface was captured to document surface changes and potential crack development. Subsequent cycles were then applied in the same manner to monitor the progressive effects of the W-D process.

2.3 *Image processing and quantitative analysis*

After each wetting cycle, the specimens were allowed to dry in a laboratory environment. Surface images were taken periodically throughout the drying process. To ensure consistent lighting and stable contrast across the sample surface, all images were taken inside a lightbox.

For separating crack regions from intact soil regions, the collected images were converted to grayscale and then binarized using a fixed threshold. However, noise in the form of isolated black spots, unrelated to actual cracks, was frequently detected on the sample surface. These irrelevant features were manually removed in a post-processing step, as illustrated in Figure 2. The resulting cleaned binary images were then used as input for the following crack analysis.

The cleaned binary images were then processed using a custom MATLAB script to obtain the geometric features of desiccation crack networks. The processing was initiated by thinning the crack network using a medial-axis transformation, which reduced each segment of the crack to a single-pixel-wide line, preserving its topology. Branch points were located and removed to isolate single crack segments. For each segment, the actual length and average width were calculated from the calibrated pixel-to-millimeter ratio, based on the known physical dimensions of the sample surface (118 × 118 mm^2).

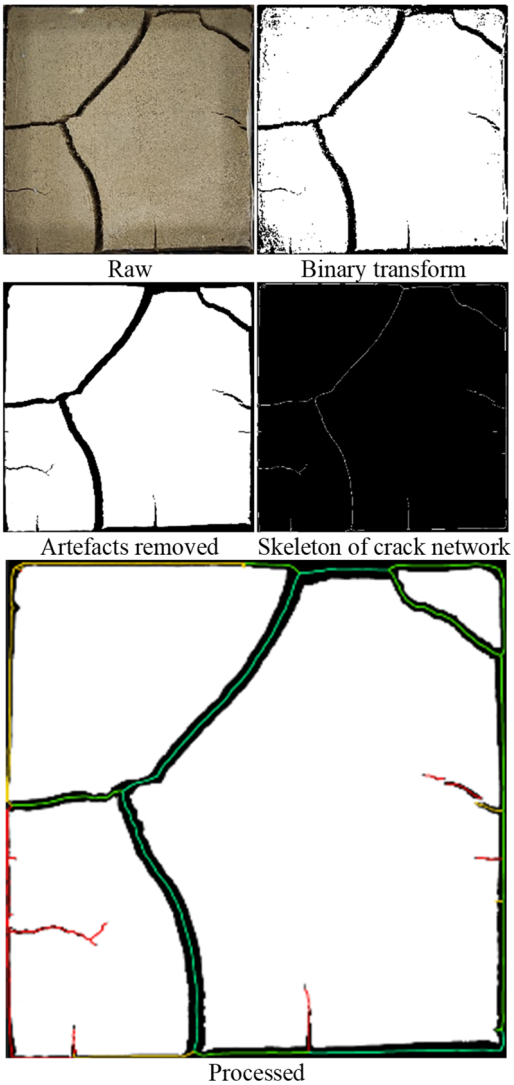

Figure 2. The image processing sequence for analyzing desiccation cracks.

The crack segments were then classified into 15 predefined width intervals (e.g., 0–0.1 mm, 0.1–0.2 mm, etc.), and each category was assigned a different RGB color code. In addition to qualitative inspection, a color-coded overlay image was generated to facilitate quantitative interpretation. The crack intensity factor (CIF), which is defined as the ratio of the total

crack area to the specimen's surface area, was also calculated by the MATLAB script. A sample output image and the corresponding classification scheme are presented in Figure 2.

3 RESULTS AND DISCUSSION

3.1 *Effect of bentonite content and wetting-drying cycles on crack intensity factor*

The formation of desiccation cracks in bentonite-sand mixtures under repeated W-D cycles was quantitatively evaluated by the CIF. Figure 3 shows the CIF development over six days for both the first and second W-D cycles. As shown in Figure 3, CIF increased incrementally throughout the first W-D cycle, to approximately 12% on day six. There was a significant CIF increase in the second cycle, where values were in excess of 18%, indicating that desiccation cracking was more intensified under repeated cycling. The CIF in the second cycle is higher than that of the initial cycle, demonstrating the irreversible nature of clay shrinkage and the structural damage in the soil matrix under repeated wetting and drying. As a result, this makes the soil more vulnerable to larger surface deformations with increasing crack area and intensity. These findings confirm that crack extension in bentonite barriers is cumulative, and this emphasizes the need to incorporate repeated exposure to the W-D cycles in long-term performance calculations.

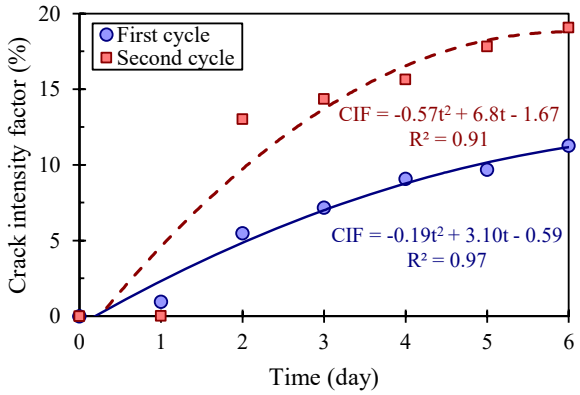

Figure 3. The variation of the crack intensity factor (CIF) with time during the first and second W-D cycles.

3.2 *Desiccation crack Evolution in repeated wetting–drying cycles*

Figure 4 shows the pattern and distribution of cracks following its first W-D cycle. The network of cracks is well established by Day 5, with wide, interlinked fissures clearly visible in the binary and classified images. The classified image shows that there is a range of crack widths, with a number of large cracks making up most of the crack area.

Figure 5 presents the cumulative crack length as a function of crack width for Days 1, 2, and 5. On Day 1, most of the cumulative length is related to the fine cracks, particularly the cracks narrower than 1.5 mm, with a total length of approximately 220 mm. By Day 2, the overall crack length increases dramatically to above 650 mm, and this is mostly because of the growth of cracks with widths in the 1.5 to 3 mm range. By Day 5, total crack remains stable, indicating most crack extension is complete, even though the curve extends out further to greater crack widths, indicating more widening has occurred. This is an indication that cracks in subsequent stages of drying do not grow in length considerably but tend to widen, especially in already existing cracks.

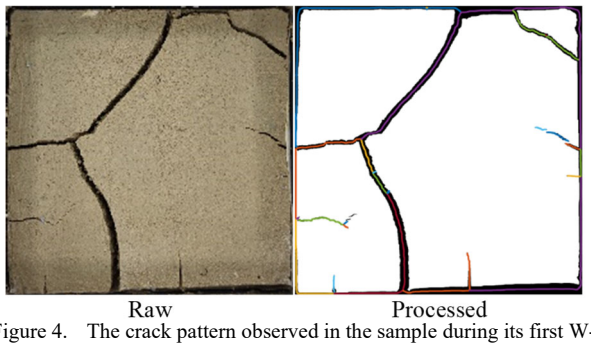

Figure 4. The crack pattern observed in the sample during its first W-D cycle, with corresponding binary and classified images for Day 5.

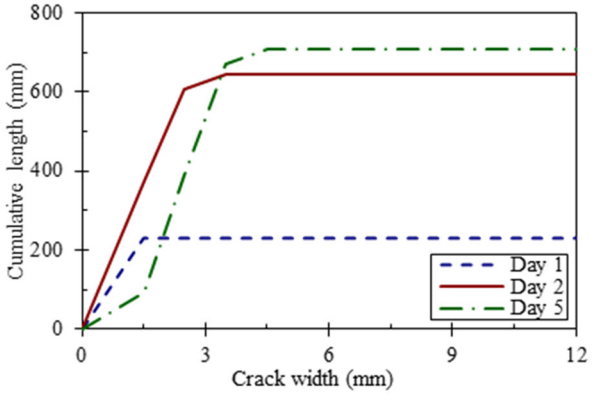

Figure 5. Enhancement of cumulative crack length with increasing crack width during the first W-D cycle.

Figure 6 illustrates the crack pattern and width distribution at the second W-D cycle. The crack network on Day 5 is more developed compared with the first cycle network. The classified and binary images clearly mark the reactivation and growth of the previously developed cracks to form a web-like network.

Figure 7 presents the cumulative crack length as a function of crack width for Days 1, 2, and 5. No visible cracks are seen on Day 1, indicating that the specimen was still intact under the condition of early drying. By Day 2, the cracks evolve extremely fast, and the cumulative crack length increases dramatically to approximately 750 mm, most of which are concentrated between the 1.5 to 3 mm width range. Between Day 2 and Day 5, the total crack length remains more or less constant, but the distribution shifts toward wider widths, revealing the widening of pre-existing cracks. These observations confirm that in the second cycle, previously formed cracks tend to reopen and expand more readily, resulting in more severe desiccation cracking.

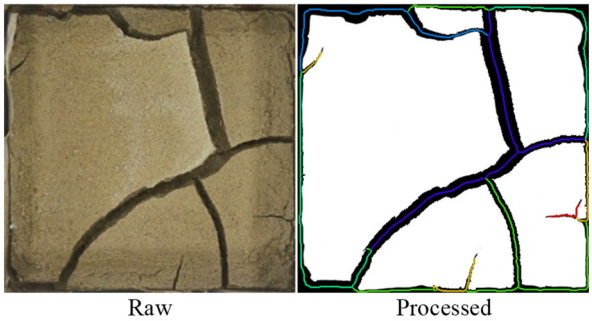

Figure 6. The crack pattern observed in the sample during the second W-D cycle, with corresponding binary and classified images for Day 5.

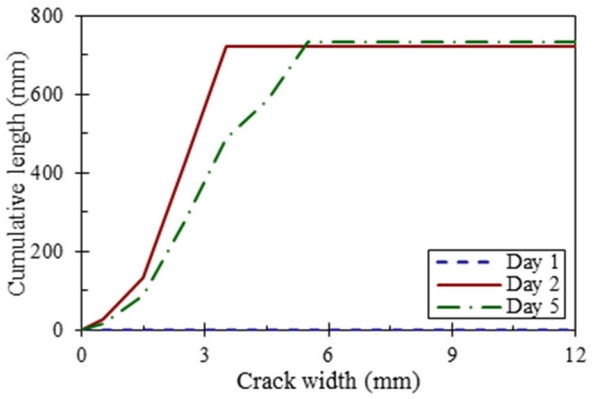

Figure 7. Enhancement of cumulative crack length with increasing crack width during the second W-D cycle.

4 CONCLUSION

This study investigated the progression and formation of desiccation cracks in a bentonite-sand sample subjected to multiple W–D cycles. Characterization of the development of cracks in terms of CIF, total length, and width distribution was performed through a combination of laboratory testing and image-based analysis. Accordingly, the following findings may be concluded:

- The CIF began to increase gradually over the initial W–D cycle, even going as high as approximately 12% on day 6. However, during the second cycle, the increase was sharper, with CIF reaching above 18%, indicating that desiccation cracking becomes intensified due to successive W-D cycles. This confirms the irreversible and cumulative nature of cracking in bentonite-sand mixtures.
- Image analysis revealed that the majority of crack development, in terms of length, occurs during the first few days of drying, i.e., between day 1 and day 2. While crack length remains relatively stable, the existing cracks tend to widen.
- During the second W–D cycle, the pre-existing cracks not only reformed but also experienced a significant rise in width. On the other hand, the overall crack length remained almost unchanged. This mechanism of reactivation highlights the structural vulnerability of bentonite-sand mixtures to repeated W–D cycles.
- In conclusion, the findings confirm that the generation of the crack process in sand–bentonite systems is both cyclic-dependent and progressive. Once a crack network is established, future cycles lead primarily to widening rather than the formation of new cracks. These findings emphasize the importance of considering repeated W–D exposure in long-term design and performance assessment of barriers, e.g., landfill liners, based on bentonite hydraulic sealing.

5 REFERENCES

Arabchobdar, F., Sadeghi, H., Gholami, M., and Alipanahi, P. 2024. Multi-directional deformation and hydraulic conductivity of expansive soils subjected to freeze-thaw cycles from three distinct initial saturation levels. Journal of Rock Mechanics and Geotechnical Engineering.

Cheng, Q., Tang, C.S., Zeng, H., Zhu, C., An, N., and Shi, B. 2020. Effects of microstructure on desiccation cracking of a compacted soil. Engineering Geology 265, 105418.

Gholami, M., Sadeghi, H., and Alipanahi, P. 2025. Anisotropic hydraulic conductivity of as-compacted, bare and vegetated soils. Géotechnique 75(6), 773–786.

Ikeagwuani, C.C., and Nwonu, D.C. 2019. Emerging trends in expansive soil stabilisation: A review. Journal of Rock Mechanics and Geotechnical Engineering 11(2), 423–440.

Joshaghani, M., and Ghasemi-Fare, O. 2021. Exploring the effects of temperature on intrinsic permeability and void ratio alteration through temperature-controlled experiments. Engineering Geology 293, 106299.

Julina, M., and Thyagaraj, T. 2020. Combined effects of wet-dry cycles and interacting fluid on desiccation cracks and hydraulic conductivity of compacted clay. Engineering Geology 267, 105505.

Ladd, R.S. 1978. Preparing test specimens using undercompaction. Geotechnical Testing Journal 1(1), 16–23.

Namadi, A., Hassanlourad, M., Motlagh, A.H., Alipanahi, P., Sadeghi, H., and Ahmadihosseini, A. 2020. Impact of lead and sodium carbonate on consolidation and hydraulic properties of clayey sand. GeoVirtual 2020, Resilience and Innovation.

Ruiz, A.I., Fernández, R., Jiménez, N.S., Rastrero, M.R., Regadío, M., de Soto, I.S., and Cuevas, J. 2012. Improvement of attenuation functions of a clayey sandstone for landfill leachate containment by bentonite addition. Science of the Total Environment 419, 81–89.

Sadeghi, H., and Alipanahi, P. 2020. Saturated hydraulic conductivity of problematic soils measured by a newly developed low-compliance triaxial permeameter. Engineering Geology 278, 105827.

Sadeghi, H., Gholami, M., Alipanahi, P., and Song, D. 2024. The influence of isotropic loading and unloading on anisotropic evolution of saturated hydraulic conductivity of bentonite-sand mixtures in a cube triaxial permeameter. Engineering Geology 331, 107454.

Sadeghi, H., Kohal, F.Y.B., Gholami, M., Alipanahi, P., and Song, D. 2023. Hydro-mechanical modeling of a vegetated slope subjected to rainfall. E3S Web of Conferences 382, 13004.

Sanchez, M., Atique, A., Kim, S., Romero, E., and Zielinski, M. 2013. Exploring desiccation cracks in soils using a 2D profile laser device. Acta Geotechnica 8(6), 583–596.

Tang, C., Shi, B., Liu, C., Zhao, L., and Wang, B. 2008. Influencing factors of geometrical structure of surface shrinkage cracks in clayey soils. Engineering Geology 101(3–4), 204–217.

Tang, C.S., Shi, B., Cui, Y.J., Liu, C., and Gu, K. 2012. Desiccation cracking behavior of polypropylene fiber–reinforced clayey soil. Canadian Geotechnical Journal 49(9), 1088–1101.

Tang, C.S., Wang, D.Y., Zhu, C., Zhou, Q.Y., Xu, S.K., and Shi, B. 2018. Characterizing drying-induced clayey soil desiccation cracking process using electrical resistivity method. Applied Clay Science 152, 101–112.

Tran, D.K., Ralaizafisoloarivony, N., Charlier, R., Mercatoris, B., Léonard, A., Toye, D., and Degré, A. 2019. Studying the effect of desiccation cracking on the evaporation process of a Luvisol – From a small-scale experimental and numerical approach. Soil and Tillage Research 193, 142–152.

Wan, Y., Xue, Q., Liu, L., and Wang, S. 2018. Relationship between the shrinkage crack characteristics and the water content gradient of compacted clay liner in a landfill final cover. Soils and Foundations 58(6), 1435–1445.

Yan, A., Wu, K., and Zhang, X. 2002. A quantitative study on the surface crack pattern of concrete with high content of steel fiber. Cement and Concrete Research 32(9), 1371–1375.

Yazdani, F., Alipanahi, P., and Sadeghi, H. 2024a. A comparative study of environmental and economic assessment of vegetation-based slope stabilization with conventional methods. Journal of Environmental Management 359, 121002.

Yazdani, F., Sadeghi, H., Alipanahi, P., Gholami, M., and Leung, A.K. 2024b. Evaluation of plant growth and spacing effects on bioengineered slopes subjected to rainfall. Biogeotechnics 2(2), 100080.

Yu, Z., Eminue, O.O., Stirling, R., Davie, C., and Glendinning, S. 2021. Desiccation cracking at field scale on a vegetated infrastructure embankment. Géotechnique Letters 11(1), 88–95.

Zhang, T., Deng, Y., Cui, Y., Lan, H., Zhang, F., and Zhang, H. 2019. Porewater salinity effect on flocculation and desiccation cracking behaviour of kaolin and bentonite considering working condition. Engineering Geology 251, 11–23.